Journal of Labelled Compounds and Radiopharmaceuticals
J Label Compd Radiopharm 2007; **50**: 1072–1087.
Published online 1 October 2007 in Wiley InterScience
(www.interscience.wiley.com). DOI: 10.1002/jlcr.1382

JLCR

Review Article

Isotopic labelling in the study of organic and organometallic mechanism and structure: an account

GUY C. LLOYD-JONES* and M. PAZ MUÑOZ

The Bristol Centre for Organometallic Catalysis, School of Chemistry, University of Bristol, Cantock's Close, Bristol BS8 1TS, UK

Received 5 April 2007; Accepted 11 April 2007

Abstract: An account of the use of stable isotopes (^{2}H, ^{13}C, ^{15}N, ^{18}O, ^{34}S) for the study of organic and organometallic reaction mechanism and structure, by way of kinetic determinations and modelling, NMR spectroscopy and mass spectrometry is presented. The techniques discussed include use of kinetic isotope effects, label-facilitated nOe experiments, cross-over experiments, stereoisotopochemical analysis, label-facilitated NMR analysis of enantiomers using chiral-shift reagents and NMR in chiral liquid crystal matrices. The reactions in which these tools have been applied are β-H elimination in Pd-σ-alkyl complexes, the Bayliss–Hilman reaction, C–H insertion of stable carbenes, ring-closing metathesis reactions, palladium-catalysed hydrosilyation, palladium-catalysed cycloisomerization, anionic thia-Fries rearrangements, synthesis of proton sponges and their nitrogen stereodynamics, and transition metal (Pd, Mo) catalysed allylic alkylation. Copyright © 2007 John Wiley & Sons, Ltd.

Keywords: isotopic desymmetrization; stereochemistry; reaction mechanism; organometallics; catalysis

Introduction

This paper highlights selected aspects of the research programmes conducted in the author's (GCLJ) laboratories over the last decade. The theme that unites the work presented is the use of stable isotopic labelling (^{2}H, ^{13}C, ^{15}N, ^{18}O and ^{34}S) to facilitate the investigation of structure and mechanism in organic and organometallic reactions. The choice of material selected for coverage is, quite naturally, biased by the author's perspective as to those topics where labelling provided the most insight into the problem in hand and also by the limitations of space inherent in an overview of this kind.

The investigations routinely have involved organic or organometallic synthesis, NMR or MS analysis and the measurement and simulation of reaction kinetics or product distribution analysis. Without doubt many of these techniques are familiar, or indeed routine, to the reader of *J Label Compd Radiopharm*. Nonetheless, we hope that the reader will find interest in the discussion of the strategy of the installation and deployment of the isotopic labels. On occasion, where we have strayed beyond the boundaries of routine techniques, in particular with NMR spectroscopic methodology, the emphasis of the description is as much on the technique as it is the strategy. The topics that we have chosen for this account have been subdivided into three sections, based on the type of information that we sought to attain through deployment of the isotopic label: (i) the mode of cleavage of a particular bond probed by *kinetic isotope effects* (KIEs), (ii) the *molecularity* of individual steps in a reaction sequence and (iii) *cryptostereochemical* issues probed by NMR through isotopic desymmetrization techniques.

Deuterium kinetic isotope effects

In this first section we report on three studies where the basics of the mechanism of the reaction of interest have already been elucidated and where the process of interest is the mode of cleavage of one particular bond in the overall sequence. In such cases, the information was deduced by comparison of the magnitude of the experimental deuterium KIE with that anticipated, on the basis of precedent, to be associated with this step. In the second two examples the distinction is clear, however, in the first we were misled for some considerable time because we did not appreciate that the

*Correspondence to: Guy C. Lloyd-Jones, The Bristol Centre for Organometallic Catalysis, School of Chemistry, University of Bristol, Cantock's Close, Bristol BS8 1TS, UK. E-mail: jones@bris.ac.uk, guy.lloyd-jones@bris.ac.uk

observed KIE was not that attending the step in question.

An unusually large primary-KIE accompanying a syn-β-H elimination in a σ-alkyl-Pd complex[1]

As part of our ongoing studies into the mechanism of the cycloisomerization of dienes by transition metal catalysts,[2] we identified Pd-σ-alkyl complex, **1a**, as a key intermediate in a pre-catalyst activation process.[3] Complex **1a** is unusually stable for a σ-alkyl metal bearing *syn*-beta-hydrogens (β-H), but does undergo β-H elimination in the presence of a base such as Proton Sponge (**2**) to yield the triene **3a** (Scheme 1). In order to distinguish between a *syn* and *anti* mechanism for this elimination we probed the primary KIE attending this process, known to be large (k_H/k_D ca. 6–7) for *anti*[4] and small (k_H/k_D ca. 2–3) for *syn* elimination. An unusually large primary k_H/k_D value (6 ± 1) in the competition of **1a** and the ^{2}H-labelled complex **1b** suggested a general base-catalysed *anti*-β-H elimination. However, subsequent diastereospecific ^{2}H-labelling (**1c**, **1d**) permitted unambiguous study of the stereochemistry, and also perturbed the *E*/*Z* partitioning through the KIE.

A careful study of the kinetics and products (**1cd** → **3cd**) showed that reaction proceeded not by an *anti* elimination involving **1** + **2**, by instead a stepwise mechanism involving a rapidly reversible *syn*-β-H elimination coupled to Pd–H deprotonation by **2** (Scheme 2), to give an NMR-observable Pd(0) complex of **3**. The coupling of the second *prim*-KIE to the β-H elimination *equilibrium* gives rise to the misleadingly large *net* k_H/k_D values.

Reevaluation of the mechanism of the Baylis–Hillman reaction (BHR)[5]

The BHR has long fascinated organic chemists as it assembles two simple species to generate an enone-allylic alcohol.[6] Reaction is facilitated by nucleophilic catalysts, such as amines or phosphines, and kinetic studies support the mechanism shown in Scheme 3. The RLS (rate-limiting step) is commonly accepted as being Step 2, based for example on the lack of a primary KIE when the 'Michael-acceptor' α-carbon is deuterated.[7] However, the accelerating effect of protic solvents and substantial *autocatalysis* in the absence of them led us to propose that the rate-limiting event is Step 3, which involves proton transfer from the α-keto methine to the alkoxide in the zwitterionic intermediate **4**, Scheme 3. To distinguish this from the classical mechanism in which Step 2 is accelerated by activation of the aldehyde by hydrogen bonding to the protic solvent, **5**, Scheme 3, we probed for a KIE in the initial phase of the reaction before product concentration builds up and thus proton transfer becomes increasingly efficient.

A competition experiment followed by ^{1}H NMR between an equimolecular mixture of **6** and *d*-**6** (Scheme 3) showed an increase of the mole fraction of *d*-**6** in the early stages of the reaction, which corresponded to a primary KIE if Step 3 is the RLS. By modelling the kinetics of this process, we were able to extract a KIE $= 5 \pm 2$ for Step 3, which is attenuated to 1 when autocatalysis becomes substantial, consistent with a change in the RLS from Step 3 to Step 2. This change of RLS is early in the reaction (after about 10%)

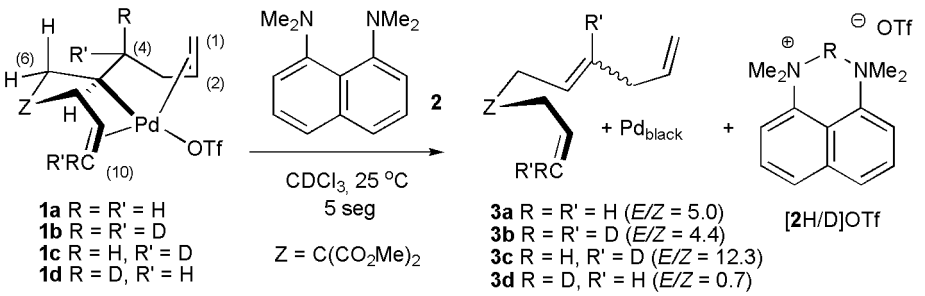

Scheme 1 Base-induced β-H elimination in Pd complex **1**.

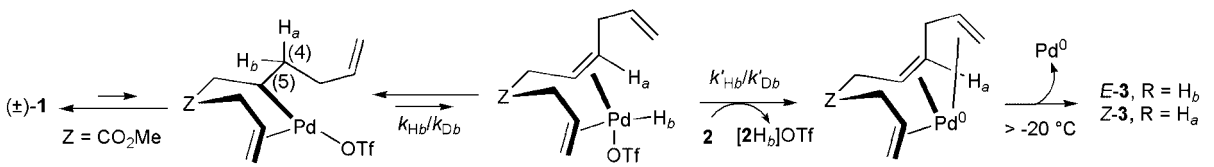

Scheme 2 Mechanism for β-H elimination in Pd complex **1**.

DOI: 10.1002.jlcr

explaining why it was overlooked in earlier studies which concentrated on the full reaction evolution.[8] These findings have considerable implications for asymmetric catalysis of the BHR, and the position of suitable hydrogen-bond donors for selective proton transfer of one of the alkoxide diastereoisomers in the presence of an aprotic solvent could led to high enantioselectivities.[9]

Intermolecular insertion of an *N,N*-heterocyclic carbene into a non-acidic C–H bond[10]

As part of a project to investigate the fascinating chemistry of *N,N*-heterocyclic carbenes (NHCs),[11] we prepared C(2)-[^{13}C]-precursors to NHC **7**. The label facilitated the detection, by ^{13}C{^{1}H} NMR, of a number of byproducts (< ca. 2.5%) arising from generation of **7** in toluene/(K-HMDS)$_2$. One such side product, which increased in proportion over a period of weeks, emerged as that arising from formal insertion into a C–H bond of the toluene (solvent) methyl group to give the aminal **8**, Scheme 4. This being the first example of such an insertion reaction of an NHC into a 'non-acidic' C–H bond, we investigated it in considerable detail.[12] The reaction was found to be catalysed by (K-HMDS)$_2$, but the relationship between the rate of insertion and the concentration of (K-HMDS)$_2$ was complex.

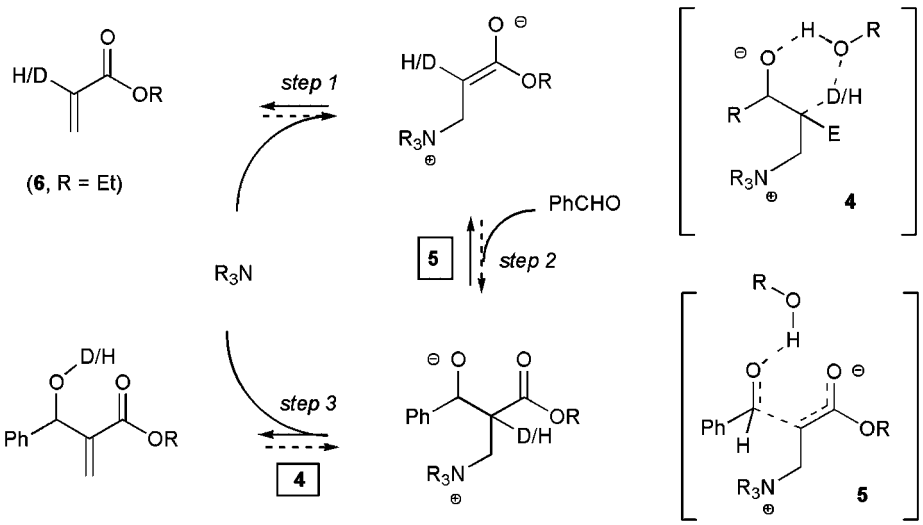

Scheme 3 Mechanisms for the Baylis–Hillman reaction (BHR).

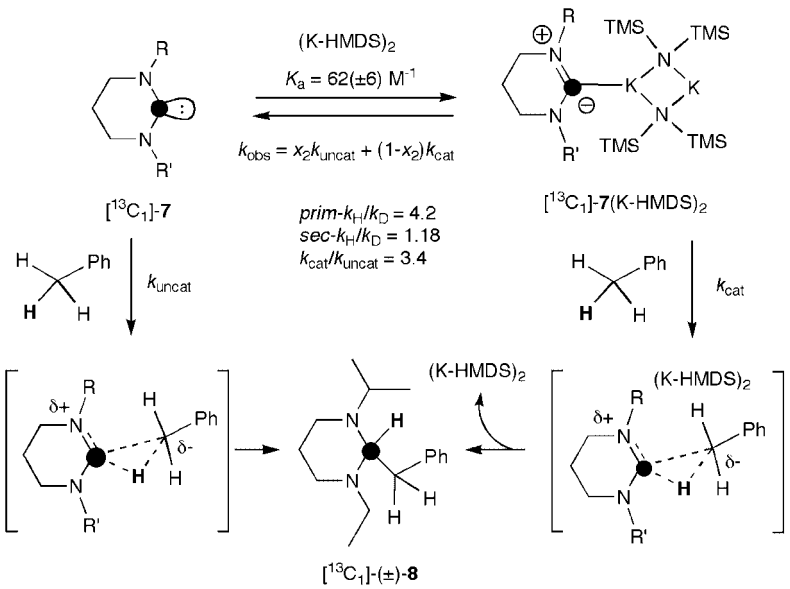

Scheme 4 Uncatalysed and catalysed C–H insertion of carbene **7**.

DOI: 10.1002.jlcr

Deuterium labelling at the toluene methyl group ([D_8]-, [D_1]-, and [D_0]-toluene) resulted in a moderate primary ($k_H/k_D = 4.2(\pm 0.6)$) and large secondary ($k_H/k_D = 1.18(\pm 0.08)$) KIEs for [D_1]-toluene in C_6D_6 and [D_0]toluene/[D_8]toluene as reactant and solvent. These values, together with rates of reaction measured for para-substituted toluenes ($\rho = 4.8(\pm 0.3)$), were consistent with a rate-limiting C–H deprotonation reaction proceeding via a late transition state. The installation of the ^{13}C-label in **7** also facilitated a careful study of the $^{13}C\{^1H\}$ NMR spectra of [$^{13}C_1$]-[D_n]-**8** arising from the deuterated toluenes, which demonstrated that the HMDS anion was not an active base in this process: there was no evidence for cross-over exchange through bulk phase H-HMDS/D-HMDS. Further study of the ^{13}C NMR shift of C(2) in **7** as a function of [(K-HMDS)$_2$] concentration revealed equilibrium complexation leading us to propose a dual-manifold mechanism involving [(K-HMDS)$_2$]-catalysed and uncatalysed processes, as shown in Scheme 4.

Molecularity

In this section we describe four reactions in which we wished to probe the molecularity of the net transformation, which, in particular for catalytic systems, can be quite opaque when one attempts to address this through measurements of the *global* reaction kinetics. Here then the use of one or more isotopic labels can be used in great effect to confirm and indeed quantify the transfer of molecular components between identical and non-identical species.

Ring-closing metathesis of enynes: Evidence for an 'Ene-then-yne' pathway[13]

The Ru-catalysed ring-closing metathesis (RCM) of enynes has been widely developed and a mechanism involving an 'yne-then-ene' sequence (cycle A, Scheme 5) is commonly postulated. When the reaction is carried out in the presence of ethylene, higher yields are obtained and side reactions such as epimerization and homo-cross-metathesis are inhibited.[14] The origin of the beneficial effect of ethylene has been ascribed to the attenuation of unproductive resting states in equilibrium with the ruthenium methylidene ([Ru] = CH_2) in the catalytic cycle. An alternative mechanism involving an 'ene-then-yne' sequence (cycle B, Scheme 5) has also been proposed[2c,15] for the RCM of enynes. Two different ^{2}H- and ^{13}C-labelling strategies have allowed us to probe the origin of the ethylene acceleration and its relationship to the mechanistic dichotomy in this reaction.

The use of stereospecifically labelled enynes (*E*)-^{2}H-**9** and (*Z*)-^{2}H-**9** provided us with evidence for an 'ene-then-yne' mechanism (cycle B, Scheme 5). Specifically, any net diastereoselectivity in the formation and breakdown of the ^{2}H-ruthenacyclo*butane* **11** intermediate, Scheme 6, will translate into *E*/*Z* selectivity in the products, as the relative configuration of the CHD and CHR centres in **11** are determined by the geometry of the alkene substrate. This is not compatible with cycle A, Scheme 5, which involves ring opening of ruthenacyclo*butene* **12** with no C-based stereogenic centres in the ring.

This 'ene-then-yne' mechanism also explained the effect of ethylene, by way of a secondary cycle (cycle Bii, Scheme 5). This possibility was investigated using a dual-substrate, dual-labelling strategy conducting the reaction under [$^{13}C_2$]-ethylene (Scheme 7). The analysis of *relative* $^{13}C/^{12}C$ incorporation in the two products (more ^{13}C is incorporated in the more accelerated substrate) confirmed that the reaction proceeded predominantly through pathway Bi/Bii under ethylene. The use of ^{2}H-labelled reference products to quantify the level of *post*-turnover

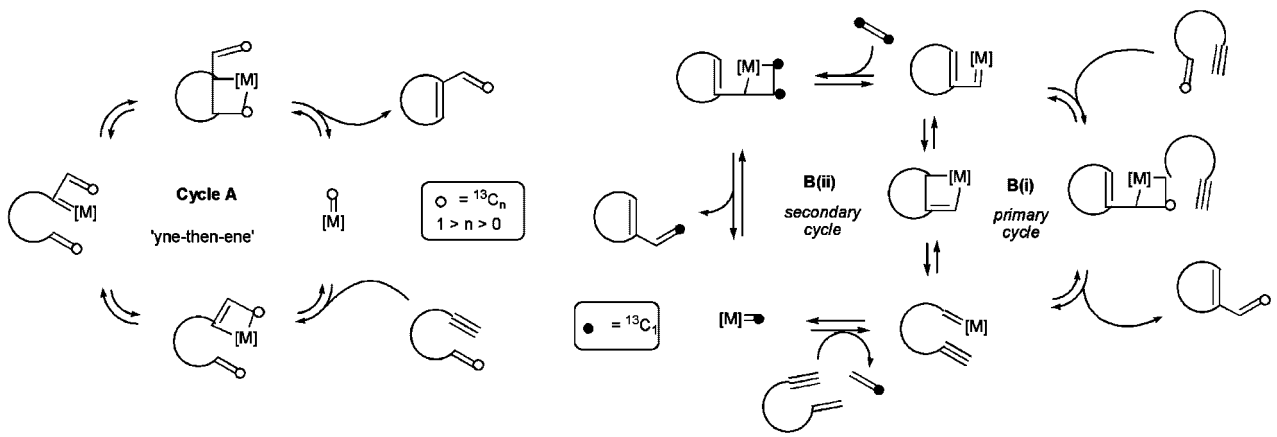

Scheme 5 Two different cycles (**A** and **B**) for Ru-catalysed enyne RCM, together with a mechanism for ethylene acceleration.

DOI: 10.1002.jlcr

incorporation, allowed comparison of $^{13}C/^{12}C$ incorporations arising through productive turnover of the catalyst.

Intermolecular chirality transfer from silicon to carbon[16]

Although the Pd-catalysed hydrosilylation of alkenes by *achiral* silanes has been studied in great detail,[17] the subtleties of the stereochemical details of the individual steps in this process remain to be explored. The mechanism for this reaction has been proposed as a 'two-silicon cycle' involving a silane-mediated pre-catalyst activation followed by a three-step propagation sequence.

The same model can be applied to the reaction with *chiral* silanes (when the silane is Si-stereogenic), where the chirality transfer from carbon to silicon can occur at one or both of two stages (Step 2 or Step 3, Scheme 8). We recently reported a mechanistic study of this process based on stereoisotopochemical probes (^2H and ^{29}Si) in catalytic cross-over experiments that validate the proposed two-silicon cycle and reveal which step (2 versus 3) gives rise to the highly efficient silicon-to-carbon chirality transfer occurring in this process.

A series of experiments using [^{13}C]-**13** and [^2H]-**13**, in which conversion and [alkene]/[Pd] were varied, were analysed by $^{29}Si\{^1H\}$ NMR, exploiting a combination of $^1J_{SiC}$ and γ-^2H isotope shifts (Scheme 9). A single kinetic model, based on the two-silicon cycle, shown

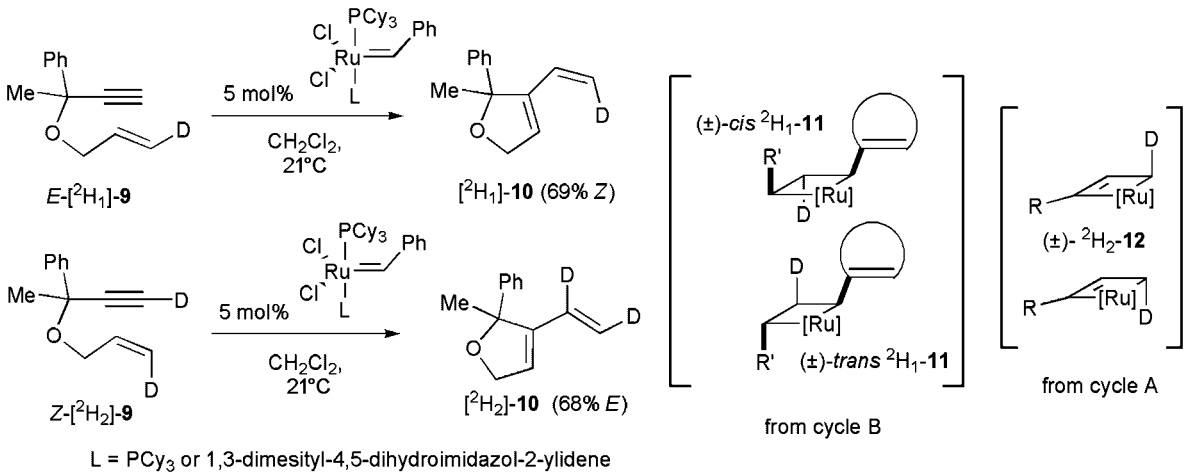

Scheme 6 RCM of stereospecifically ^2H-labelled enynes **9**.

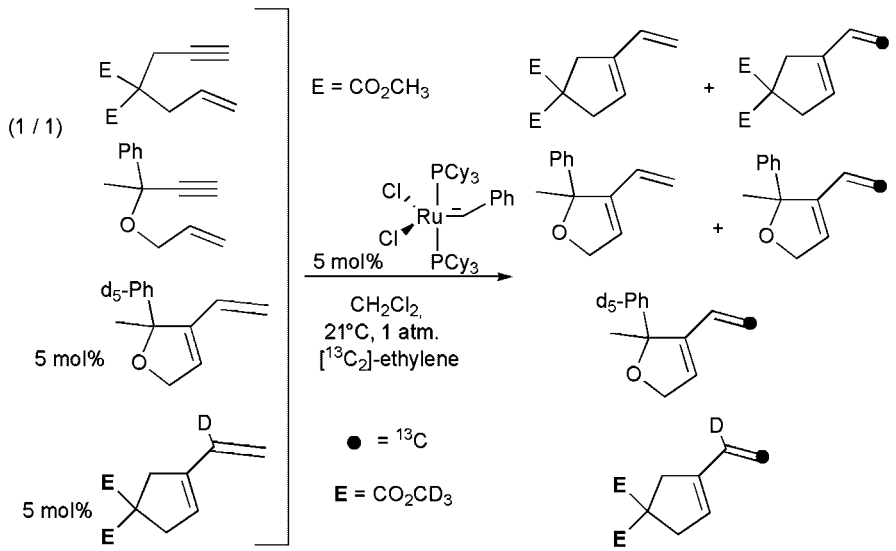

Scheme 7 A dual-substrate, dual-labelling strategy to probe for ethylene acceleration by cycle Bii (Scheme 5).

DOI: 10.1002.jlcr

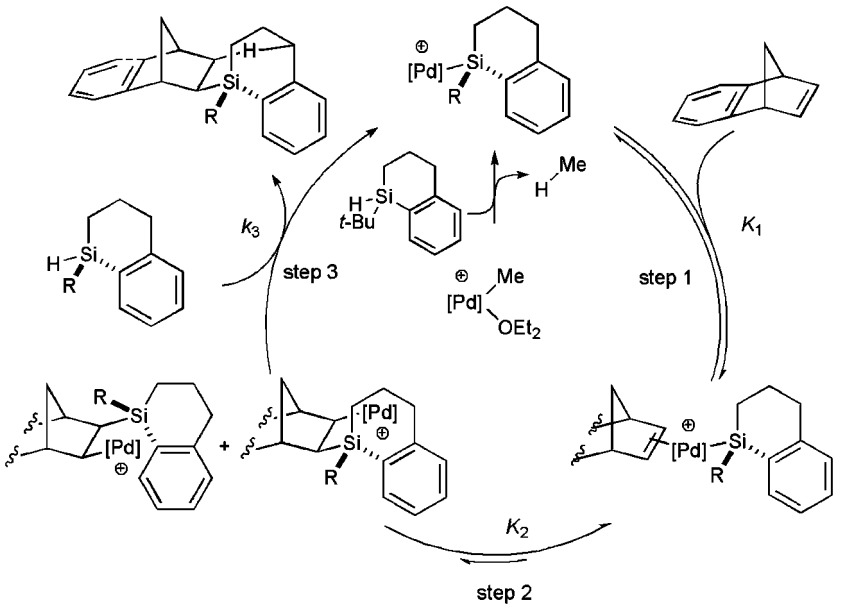

Scheme 8 A 'two-silicon cycle' for Pd-catalysed alkene hydrosilylation with highly efficient chirality transfer (Step 2).

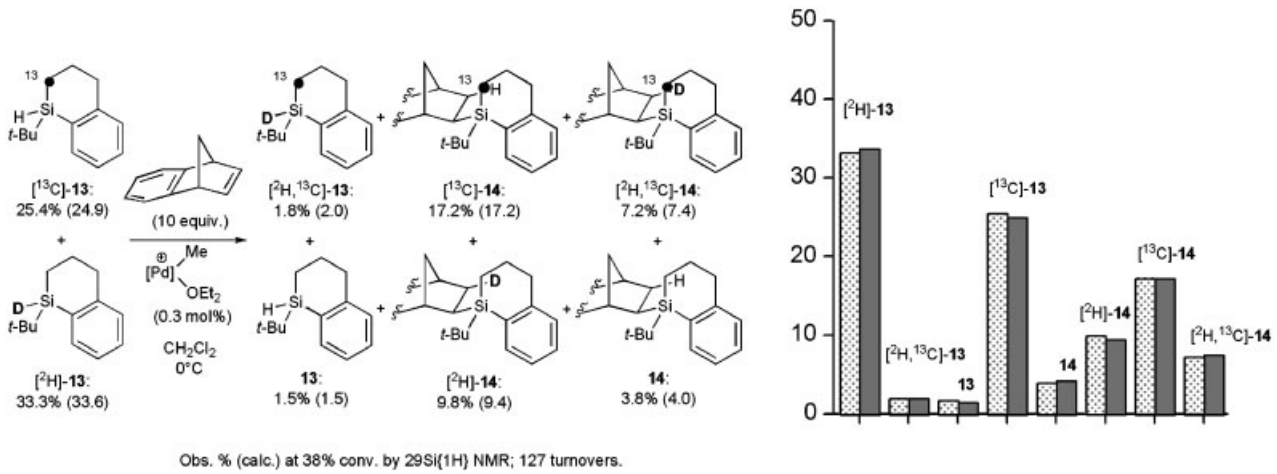

Scheme 9 Comparison of observed isotope distributions in hydrosilylation products arising from labelled silanes, with those predicted from kinetic modelling of the mechanism in Scheme 8.

in Scheme 9 in which a PKIE of 2.5 attends cleavage of Si-^{2}H in Step 3 and in which scrambling is inversely proportional to [alkene], gave an excellent fit for the ^{2}H/^{13}C distribution in the products (**14**, Scheme 9).

By analysis of the cross-over products from the reaction of (Si*R*)-**13** (97% ee) with an *achiral* ^{2}H-labelled silane we showed that the highly efficient silicon-to-carbon chirality transfer must occur in Step 2 of the mechanism outlined in Scheme 8. In addition it is found that asymmetric amplification can occur when non-racemic silane is employed. Through the use of quasiscalemic silane (non-racemic silane in which one enantiomer is isotopically differentiable from the other) we demonstrated that this arises from chirality match/mismatch effects in Step 3.

Palladium-catalysed cycloisomerization of dienes[3,18]

The transition-metal catalysed cycloisomerization of dienes is a powerful method for the synthesis of carbo- and heterocycles.[2] A variety of catalysts have been reported for this reaction and different mechanisms have been proposed. We have focussed on the Pd catalysed reaction and identified a number of pre-catalysts that give rise to different products. For

DOI: 10.1002.jlcr

example, [$(MeCN)_2$Pd(allyl)]OTf and [$(t$BuCN$)_2PdCl_2$]) give different kinetic selectivity for the cycloisomerization of **15**, which suggests (erroneously) that the mechanisms of the processes are unrelated (Scheme 10). Thus, the kinetic product from the reaction employing the cationic complex as pro-catalyst is the exo-alkene **16**, which is then isomerized to the thermodynamically more stable compounds **17** and **18**. However, the neutral, chloride-bearing complex effects an extremely selective cycloisomerization of **15** directly to **17**, without free **16** being an intermediate and without significant subsequent isomerization of the kinetic product (**17** to **18**) until complete consumption of **15**.

To study the mechanisms of these reactions, we needed to be able to track the origin and destination of the hydride migrations that we suspected took place. To do this we have developed reliable and practical synthetic routes for the synthesis of a large range of single ^{2}H-, ^{13}C- and double (^{2}H, ^{13}C)-labelled variants of **15** with defined regiochemistry and alkene geometry.

The reaction of the symmetrical and unsymmetrical labelled substrates, as well as cross-over experiments were carried out in the presence of the two different Pd-catalysts (Scheme 11).

Analysis of the labelled products by ^{1}H, ^{2}H and ^{13}C NMR, and the study of the effects of alkene substitution and alkene isomerization led us to propose a Pd-H based mechanism in both cases (Scheme 12). The difference in selectivity between the two complexes can be explained simply by the presence/absence of the chloride ion in the systems employed. In the absence of chloride ion (which blocks one coordination site on the palladium) the incoming substrate molecule can bind in a *bidentate* manner *before* departure of the product just generated. This allows the incoming substrate to capture the palladium-bound hydride, thus displacing the product.[18b]

Mechanistic studies on the anionic thia fries rearrangement[19]

The LDA-mediated rearrangement of aryl triflates to give aryl triflones was discovered in the group a few years ago[19a] and has recently been applied in the preparation of modified enantiomerically pure BINOL ligands for the asymmetric In-mediated allylation of hydrazones (up to 99% ee).[20] Problems in terms of a lack of generality of the reaction (the aryl group strongly influences the outcome) led us to conduct a detailed mechanistic study. In order to probe the molecularity of this reaction and to test if benzyne intermediates are involved, we designed a series of cross-over experiments involving aryl triflate **19** containing isotopic labels on the aromatic ring, on the sulphur, and on the phenolic oxygen.

The synthesis of the triflate ^{2}H-**19** was straightforward, starting from commercially available 4-bromo-2-chlorophenol, using the triflate to protect the phenol during Grignard reaction. The synthesis of ^{18}O-**19** was achieved using K^{18}OH, prepared *in situ*, to effect a nucleophilic aromatic substitution of fluoride on chlorofluorobenzene, thus yielding the requisite ^{18}O-phenol precursor of the triflate. However, the synthesis of the ^{34}S-labelled triflate ^{34}S-**19** was more challenging, as the only ^{34}S-starting material available to us was 100 mg of the elemental form, i.e. $^{34}S_8$, Scheme 13.

The reaction of an equimolecular mixture of ^{2}H-**19** and ^{34}S-**19** in the presence of 1 equivalent of LDA in THF was analysed by mass spectrometry (Scheme 14). The observed mass spectra and a simulation of the product distributions expected from reaction without cross-over showed a good fit, confirming an intramolecular rearrangement as opposed to an anionic chain reaction.[21]

Mass spectrometric analysis of the product of reaction of ^{18}O-**19** (85%) with LDA, showed that the

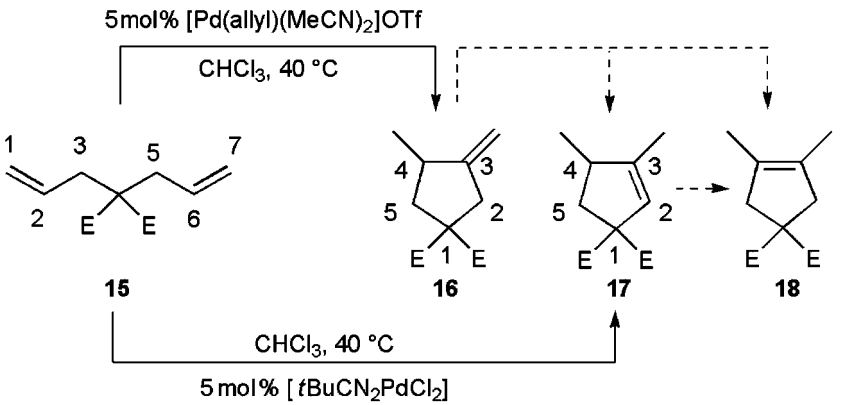

Scheme 10 Catalyst-dependent outcome in the cycloisomerization of diene **15**.

DOI: 10.1002.jlcr

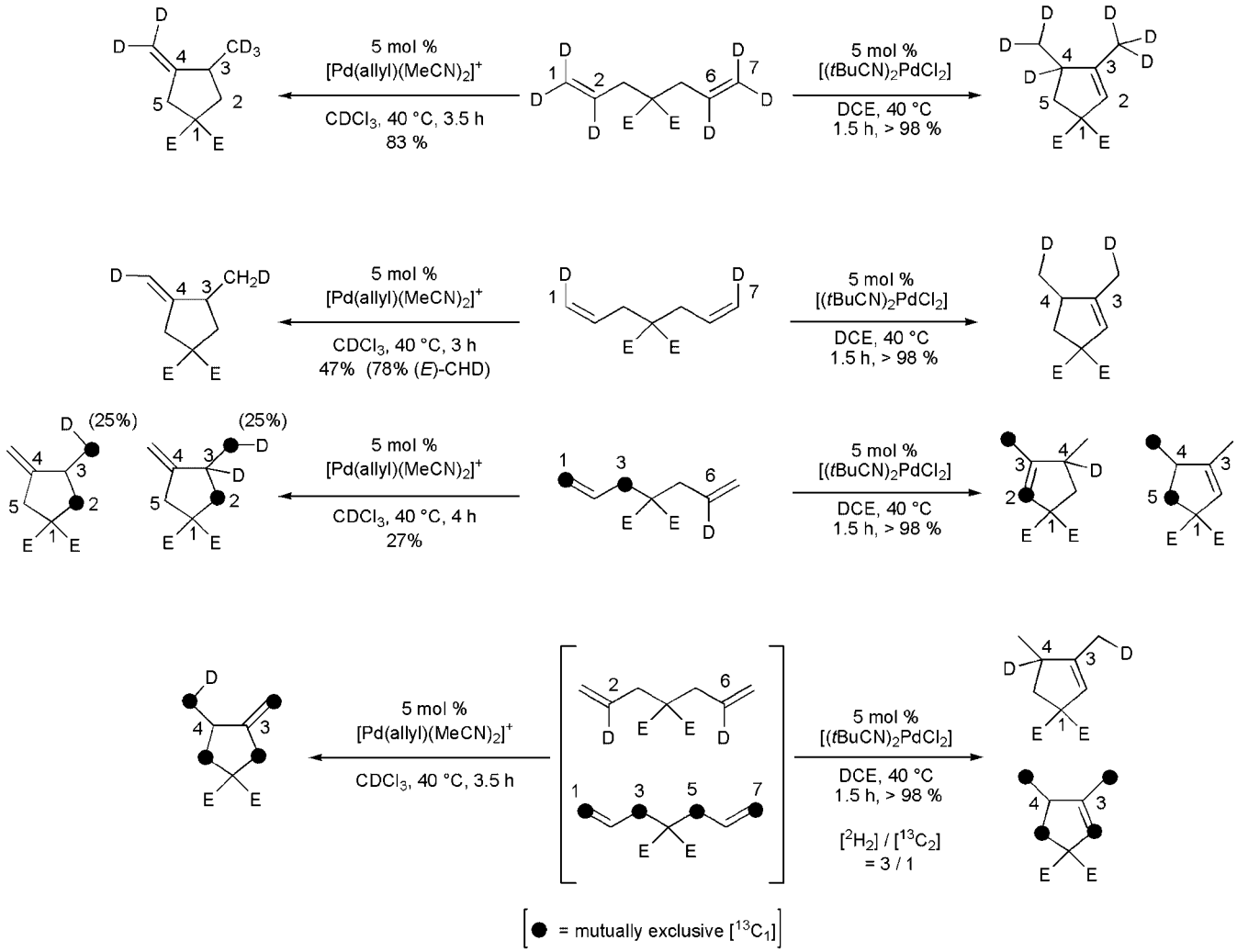

Scheme 11 Pd-catalysed cycloisomerization of single ^{2}H-, ^{13}C- and double (^{2}H, ^{13}C)-labelled variants of **15**.

daughter-ion arising from C–S cleavage and loss of SO_2CF, was ^{18}O-labelled (85%) revealing that the aryl-O bond was not broken during rearrangement and thus eliminating benzyne intermediates.

Cryptostereochemistry

In this final section the key aspect of the reaction or structures that are of interest is the stereochemistry. In the cases presented, the structures that we desired to probe contained elements of molecular symmetry (rotational or mirror plane) that serve to make interpretation, e.g. of NMR spectra, highly ambiguous. This is a common phenomenon in the study of asymmetric catalysis where C_2-symmetry is often a desirable and deliberately installed feature in chiral ligand architecture. The strategic deployment of an isotopic label can break such symmetry in a non-perturbing manner, so as to facilitate informative spectroscopic analysis.

Stereodynamics of an *N,N*-chiral 'proton sponge'[22]

The *N,N,N′,N′*-tetraalkylated derivatives of 1,8-diaminonaphthalene are characterized by their high pK_a values (ca. 12–17) and 'sluggish' behaviour: they are very poor nucleophiles and are protonated–deprotonated slowly. These features have led them being referred as 'Proton Sponges'. As part of a programme investigating H-bonding, we have studied the stereodynamics of chiral 'Proton Sponges', including their protonated forms, which have a stereogenic centre at both nitrogen atoms and can exist as three stereoisomers: a C_2 symmetric pair of enantiomers [R_NR_N/S_NS_N]-**20/20**H^+I^- or [*dl*]-**20/20**H^+I^-, and an

DOI: 10.1002.jlcr

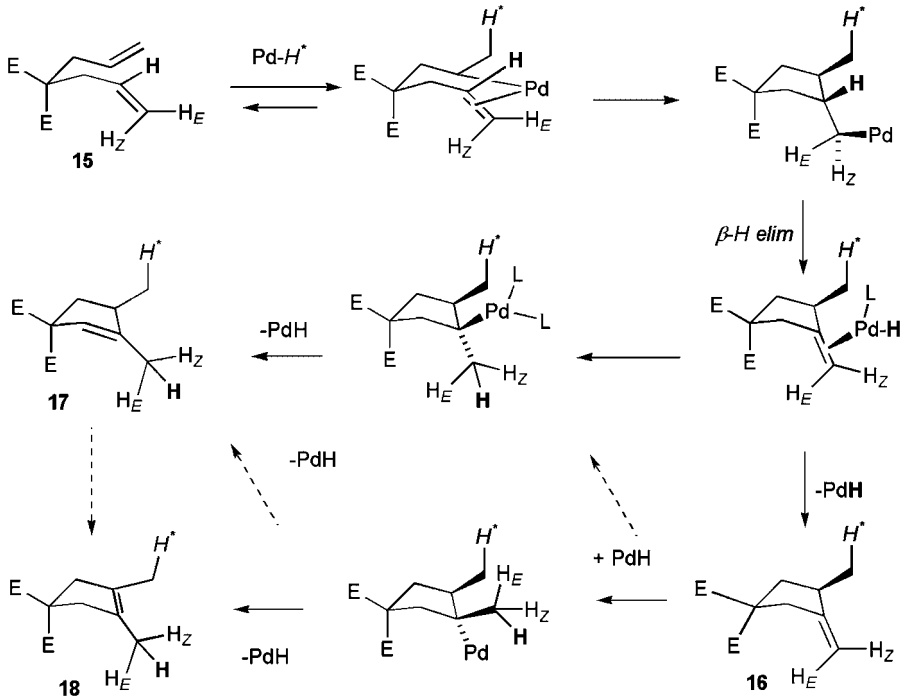

Scheme 12 Mechanism deduced for the Pd-catalysed cycloisomerization of **15**.

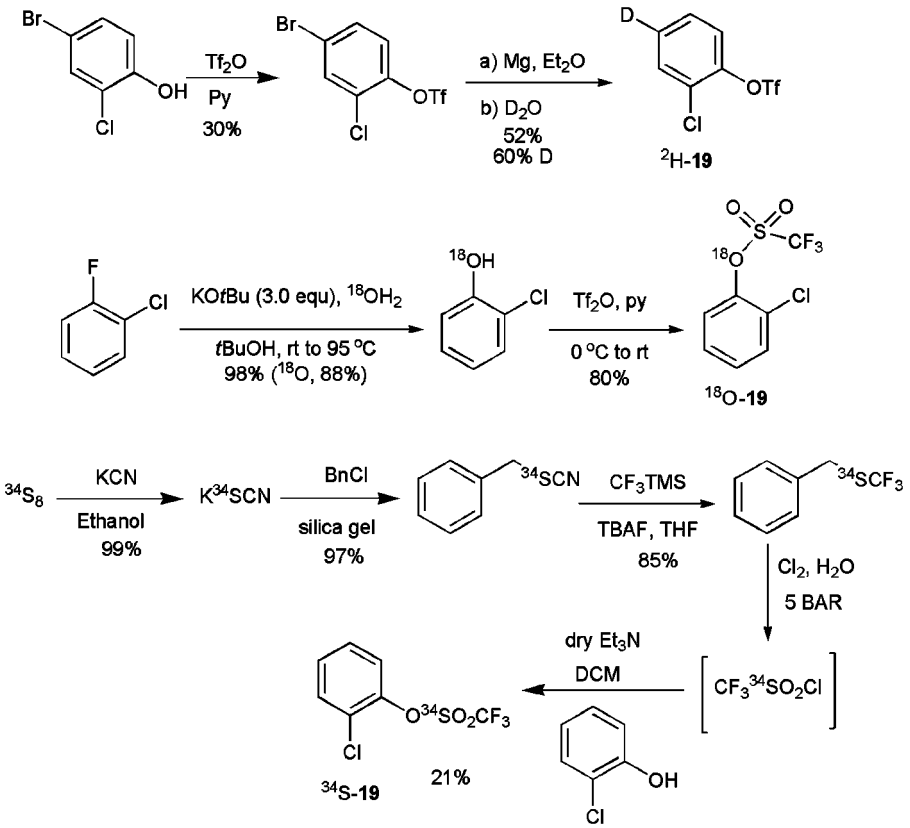

Scheme 13 Synthesis of ^{2}H-, ^{18}O- and ^{34}S-labelled isotopomers of orthochloro benzene triflate **19**.

DOI: 10.1002.jlcr

achiral form [R_NS_N]-**20/20** H^+I^- or [*meso*]-**20/20** H^+I^- (Scheme 15).

The ^1H NMR spectrum of **20** H^+I^- in $CDCl_3$ indicated that one diastereomer was present in excess (88.5:11.5) and that the stereochemistry had been efficiently 'locked', at the NMR timescale, by protonation. The [*dl*]-**20/20** H^+I^- pair was crystallized from this mixture and its structure determined by X-ray crystallography. However, on dissolution in $CDCl_3$, the two forms ([*dl*]-**20** H^+I^- and [*meso*]-**20** H^+I^-) rapidly (<5 min) equilibrated to give a constant mixture of 88.5:11.5. Both isomers gave near identical NMR spectra with only small differences in chemical shift due to the similarity and symmetry of the molecules, making stereochemical assignment troublesome. However, the major and minor isomers could be distinguished by NMR studies (^1H n.O.e. difference experiments at 500 MHz) of the isotopically desymmetrized ^{13}C-**20** H^+I^- prepared by methylation of **21** with $^{13}CH_3I$/NaH and dissolving the resultant ^{13}C-**22** in $^{12}CH_3I$ (Scheme 16).

These studies demonstrated that the thermodynamically favoured diastereomer in solution was the chiral [*dl*] form. An identical sequence of n.O.e. experiments was performed on the free base equilibrium mixture of [*dl*]- and [*meso*]-[^{13}C-**20**], obtained by treatment of ^{13}C-**20** H^+I^- with 4 M aqueous NaOH (Scheme 15), and again the [*dl*] form was assigned as the major isomer.

The rate of interconversion of [*dl*]- and [*meso*]-[^{13}C-**20**] was fast enough to allow rate constants to be determined by full band-shape analysis of the ^{13}C NMR signals arising from the well-dispersed methyl groups

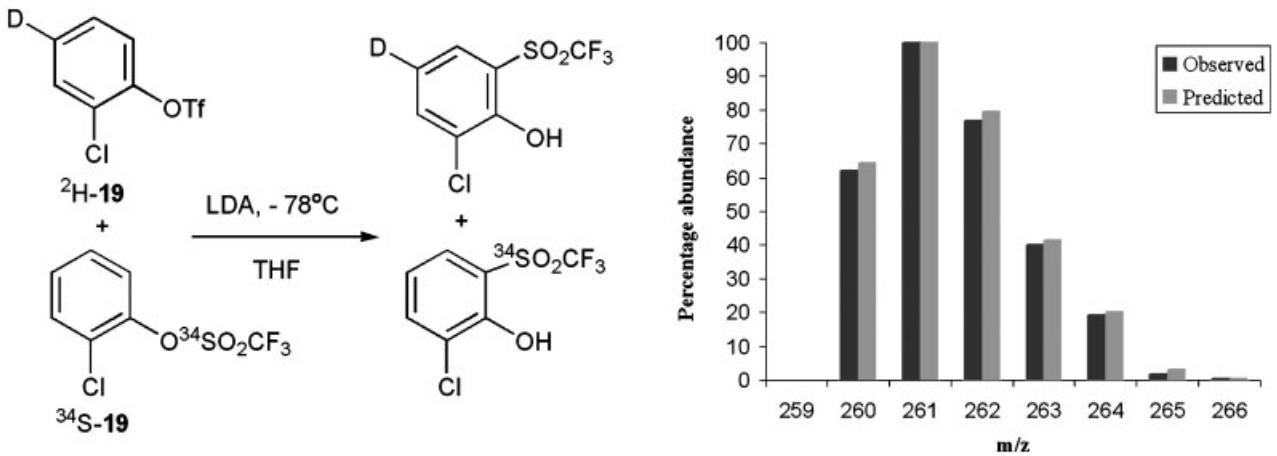

Scheme 14 Cross-over (negative) experiment with ^2H- and ^{34}S-labelled aryl triflate.

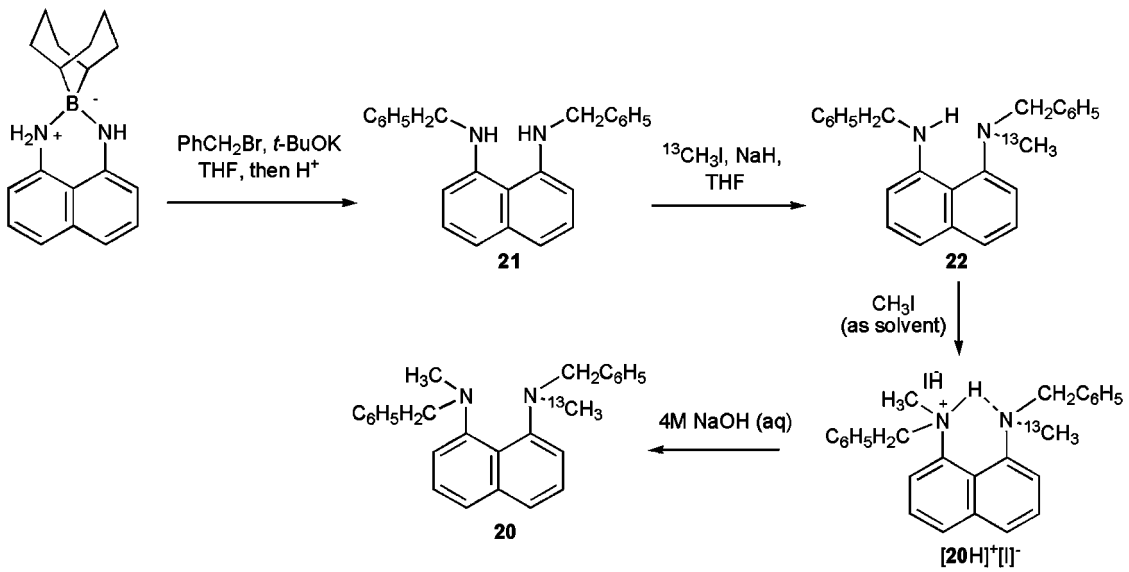

Scheme 15 Synthesis of chiral Proton Sponge **20**.

DOI: 10.1002.jlcr

at variable temperatures. The kinetics and stereodynamic processes for the interconversion of the protonated forms, [*dl*]- and [*meso*] ^{13}C-**20**H$^+$I$^-$, were again studied by ^{13}C NMR spectroscopy but using rapid temperature drop methods and selective magnetization transfer experiments. The results obtained permitted comparison of activation parameters between the *N*-stereodynamic processes involving the protonated and the free base **20**. This led us to propose a pseudo-unimolecular mechanism for the interconversion of the protonated forms, and suggested that the hydrogen bond was not of any unusual enthalpic strength or 'special character'.

To further study this hydrogen bond we prepared a number of ^{15}N-labelled 1,8-diaminonaphthalenes so that we could determine experimental values for $^{2H}J_{NN}$, the NMR coupling between the two amines *through* the hydrogen bond, (Scheme 17).

The $^{2H}J_{NN}$ values for the *non-symmetrical* free base and protonated species $^{15}N_2$-**24** and $^{15}N_2$-**24**H$^+$I$^-$ (Scheme 17) were determined directly from their ^{15}N{^{1}H} NMR spectra, where they displayed well-resolved AX systems with $^{2H}J_{NN}$ values of 3.7 and 6.70. However, for the time-average symmetrical species $^{15}N_2$-**23**, $^{15}N_2$-**23**H$^+$I$^-$ $^{15}N_2$-**25** and $^{15}N_2$-**25**H$^+$I$^-$ (Scheme 17) the ^{15}N{^{1}H} NMR spectra were not informative in terms of extracting $^{2H}J_{NN}$ values. We thus focused on their ^{13}C{^{1}H} NMR, in particular on C(1,8), where these carbons are desymmetrized from an AA′X system, by the net isotope shift of the ^{13}C (observed nucleus (C1)) versus the ^{12}C (99% non-observed nucleus (C8)) to an ABX system. Full band-shape analysis of the X-part of the spectrum allowed extraction of the $^{2H}J_{NN}$ value for each compound from a single spectrum. This approach differed from the frequency-based approach employed previously, which required a number of spectra be acquired, each at different fields.[23]

Palladium[24] and molybdenum[25]-catalysed asymmetric allylic alkylation

The asymmetric Pd-catalysed addition of nucleophiles to chiral but racemic allylic electrophiles (allylic alkylation) has become a very popular reaction to test and compare the efficacy of novel chiral ligands ('L*'). The reaction is often assumed to proceed via a *meso*-π-allyl-Pd intermediate that is desymmetrized by the chiral Pd–L* assembly. This has the effect of converging both enantiomers of substrate on a single intermediate, from which two enantiomeric products are generated. In other words, the system should have no 'memory' of which enantiomer of the substrate has been processed. However, we became interested in testing whether

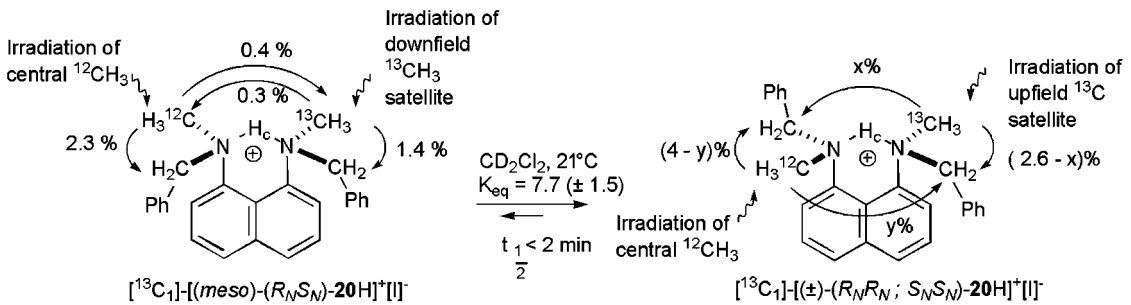

Scheme 16 Diastereoisomer assignment through n.O.e. studies facilitated by isotopic desymmetrization.

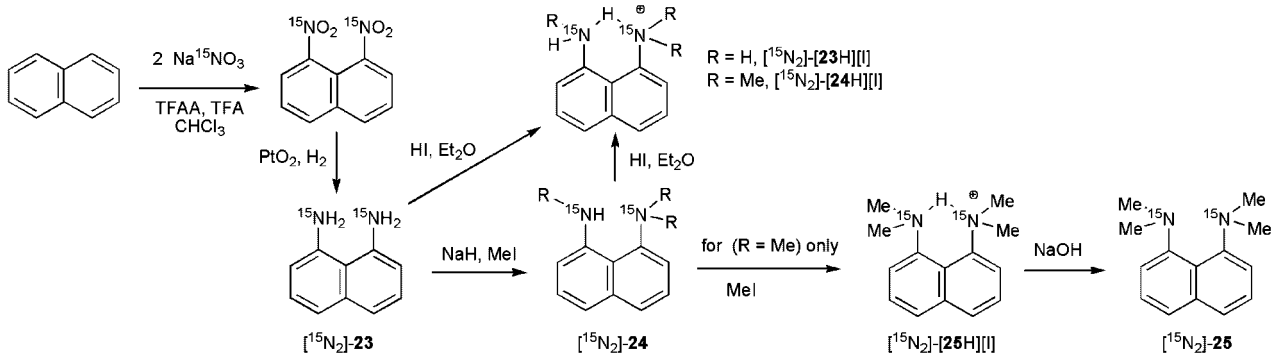

Scheme 17 Synthesis of all isomers of ^{15}N-labelled *N*-methylated 1,8-diaminonaphthalenes.

DOI: 10.1002.jlcr

this assumption was always correct, in other words is there a 'memory effect'. To do this we developed a novel stereochemical labelling method and a series of new analytical methods based on NMR techniques to study the stereochemical outcome of this reaction catalysed by Pd and Mo complexes.

To study the memory effect in the reaction of the cyclopentenyl esters of type **26**, which react with malonate carbanion to give **27**, we prepared regiospecifically (α-^{2}H-labelled cyclopentenyl substrates ($\pm$)-^{2}H -**26**a-d (>99% ^{2}H, $\alpha/\gamma \geqslant 99/1$) and also alkyl -^{18}O-labelled cyclopentenyl substrates ($\pm$)-^{18}O-**26**a-b (ca. 95% ^{18}O) (Scheme 18).

When ^{2}H-labelled **26** was reacted under Pd-catalysed allylic alkylation conditions, it gave racemic **27**, whose α/γ ratio was measured by ^{2}H NMR spectroscopy and giving an assay of the memory effect, Scheme 19, left. Mixtures of ($\pm$)-^{18}O-**26**a and ($\pm$)-^{18}O-**26**b were reacted under the same conditions to study the internal return of the nucleofuge (RCO_2) in the reaction. Finally, to study the memory effect using enantiomerically pure chiral ligands we developed a highly practical ^{13}C analytical method based on a combination of a chiral-shift reagent, (+)-Eu(hfc)$_3$ (hfc = [3-(heptafluoropropyl-hydroxymethylene-(+)-camphorate]) and ^{13}C-^{2}H isotope shifts. Once calibrated, a conventional ^{13}C{^{1}H} NMR experiment allowed simultaneous but individual measurement of the ee values of **27** arising from (*S*)-**26** and (*R*)-**26** in racemic ($\pm$)-**26**, by analysis of the C(4′)H$_2$ ^{13}C-subspectrum (Scheme 19, right).

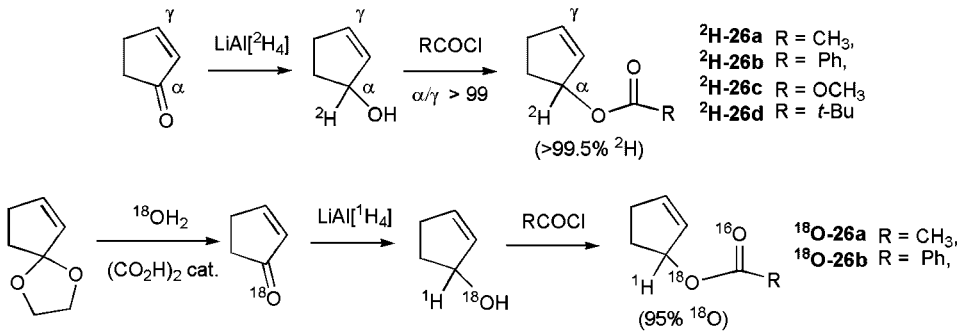

Scheme 18 Preparation of ^{2}H- and ^{18}O-labelled cyclopentenyl esters **26**.

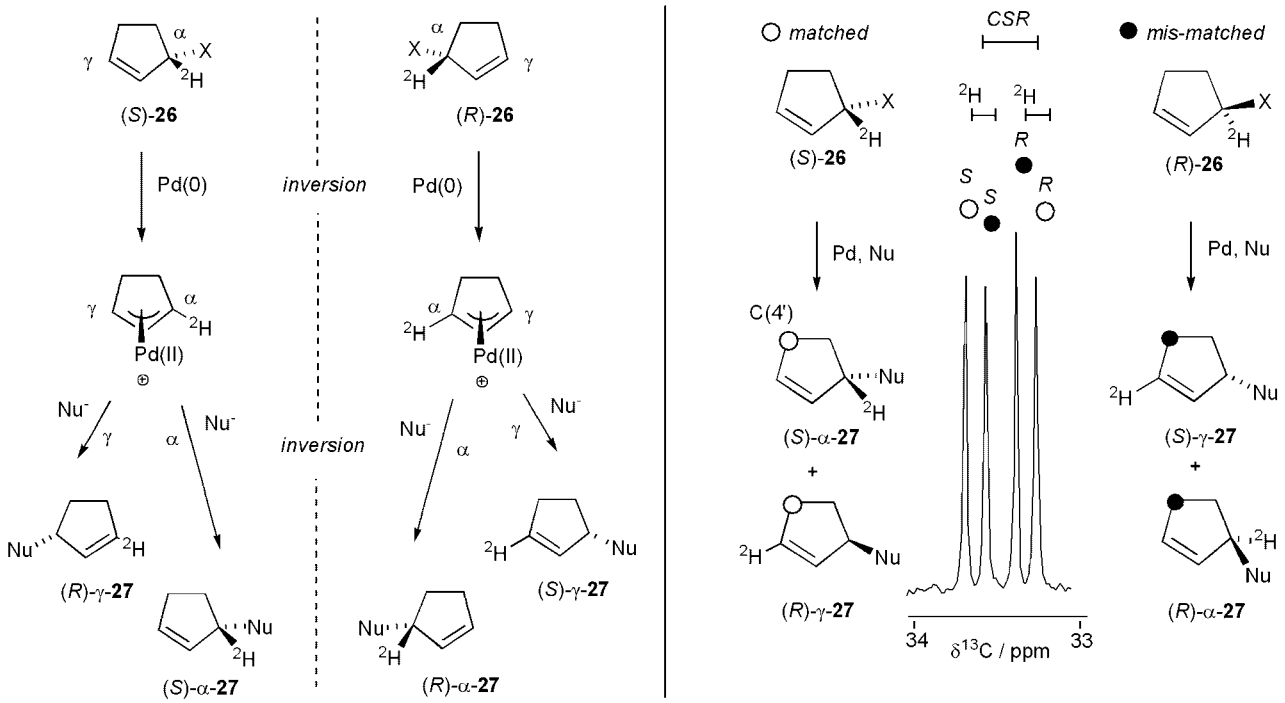

Scheme 19 Stereochemical pathways for reactions of enantiomers of ^{2}H-labelled esters **26** and the combined ^{13}C–^{2}H isotope-shift/(+)-Eu(hfc)$_3$ chiral-shift reagent method for their differentiation.

DOI: 10.1002.jlcr

This system permitted us to study the factors affecting the memory effects arising from individual enantiomers of substrate *in a racemic sample*, in the presence of different chiral ligands. The profound effect of chloride ions on memory effect and kinetic resolution was also studied using this method.

We have also studied the regiochemical memory effect on racemic *iso*-cinnamyl esters **28** (Scheme 20). In this case, we could not employ the ^{2}H-labelling technique described before for the cyclic substrates because the π-σ-π diastereofacial equilibration of the π-cinnamyl intermediates will cause the reaction to lose its stereospecificity with regard to the ^{2}H label installed at the carbon bearing the nucleofuge. As we needed two elements of stereochemical information in the labelling system to track both the regio- and stereochemical processes, we chose to deploy a ^{2}H label at the terminus of the alkene unit in **28** and with a set (*Z*)-stereochemistry. The consequence of this labelling strategy, is the possibility of the generation of six products, all of which must be resolved for simultaneous analysis of both the regioselectivity and stereoselectivity arising from both enantiomers of ($\pm$)-(1*Z*)-[^{2}H]-**28** (Scheme 20).

To analyse this mixture of compounds we used a method pioneered by Courtieu *et al.* that involves acquiring ^{2}H{^{1}H}-NMR spectra of samples dissolved in a chiral liquid crystal matrix (CLCM) consisting in a solution of poly benzyl-L-glutamate in CH_2Cl_2.[26] The anisotropy, induced through partial ordering, causes quadrupolar coupling ($\Delta|\nu_Q|$) to be manifested in the ^{2}H{^{1}H}-NMR spectrum. By using a matrix of the appropriate concentration and viscosity we were able to resolve all six components, each appearing as a doublet in the ^{2}H{^{1}H}-NMR spectrum with a different chemical shift (linear versus branched; the chemical shift anisotropy is negligible) or different quadrupolar coupling ($\Delta|\nu_Q|$). By synthesis of the reference

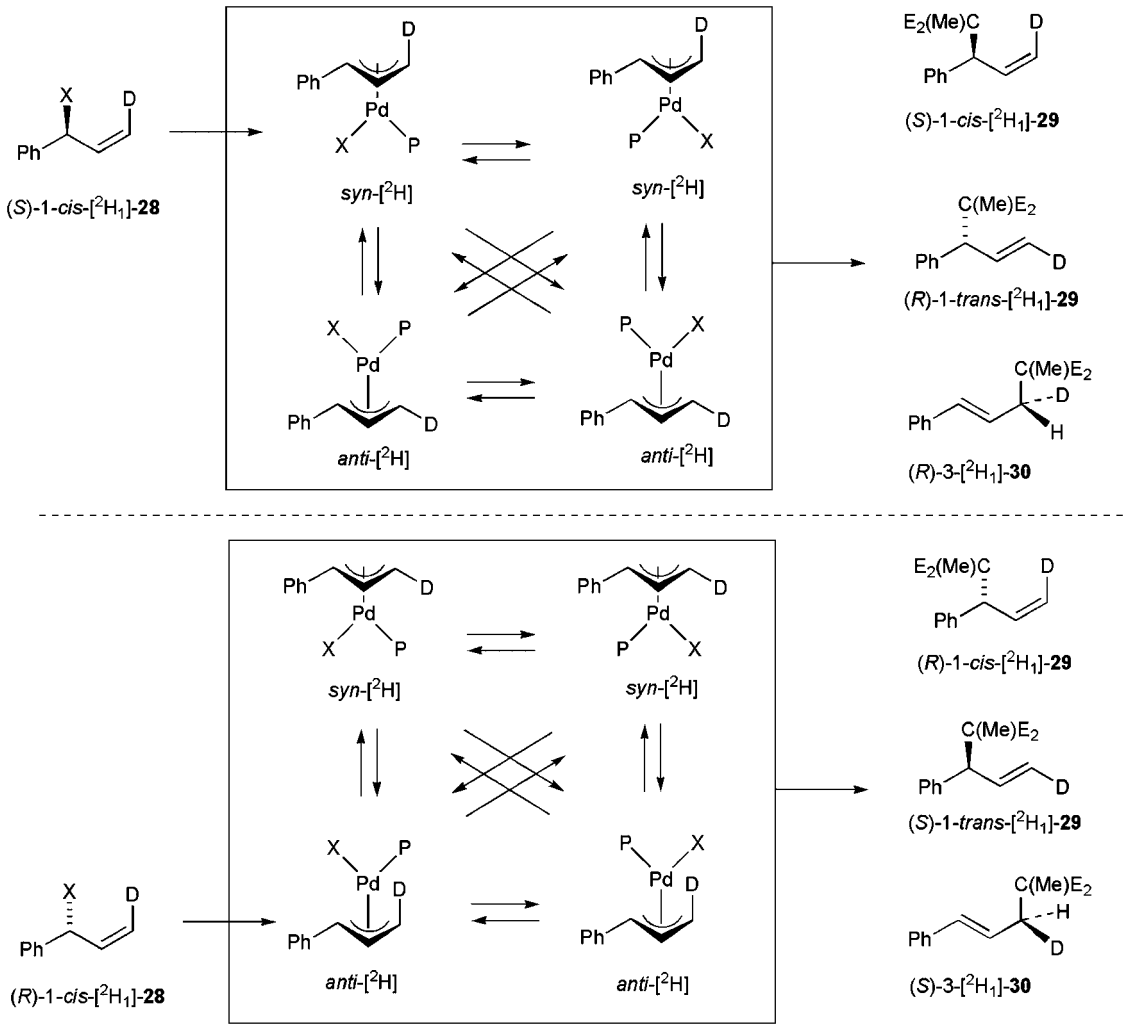

Scheme 20 Stereochemical pathways for reactions of enantiomers of ^{2}H-labelled allylic esters **28**.

DOI: 10.1002.jlcr

mixtures of the expected products (employing Pd-, Mo- and W-catalysed reactions) we were able to assign all six doublets (Scheme 21).

Compared with the Pd-catalysed reaction, the Mo-catalysed alkylation version is much less commonly applied and little is known about the mechanism. To study the stereochemical course of this reaction we have applied similar labelling strategies and NMR techniques to that we employed in the study of the Pd-catalysed reaction. The availability of the labelled substrates **28** and **31** as single ^{2}H-labelled enantiomers together with the analysis of the products of their reaction in the presence of Mo complexes by ^{2}H{^{1}H} NMR spectroscopy in the CLCM described above, allowed the stereochemical pathways of the reaction to be distinguished as either *inversion–inversion* (like Pd) or an unprecedented *retention–retention* pathway. Finally, correlation of solution phase NMR studies of intermediates with the single crystal X-ray structure of a π-allyl intermediate isolated from this reaction, together with the ^{2}H labelled analysis provided the means to conclusively establish the stereochemistry for both the oxidative addition and nucleophilic displacement steps for the Mo-catalysed allylic alkylation as being *ret–ret* (Scheme 22).

Outlook

In terms of our current and future directions in structural and mechanistic investigation of organic and organometallic reactions, stable isotopic labelling will not just continue to play a pivotal role, but will increase in scope of application and technique. Moreover, as our experience with isotopic label installation increases, and our confidence grows accordingly, we have become ever more ambitious in terms of the types

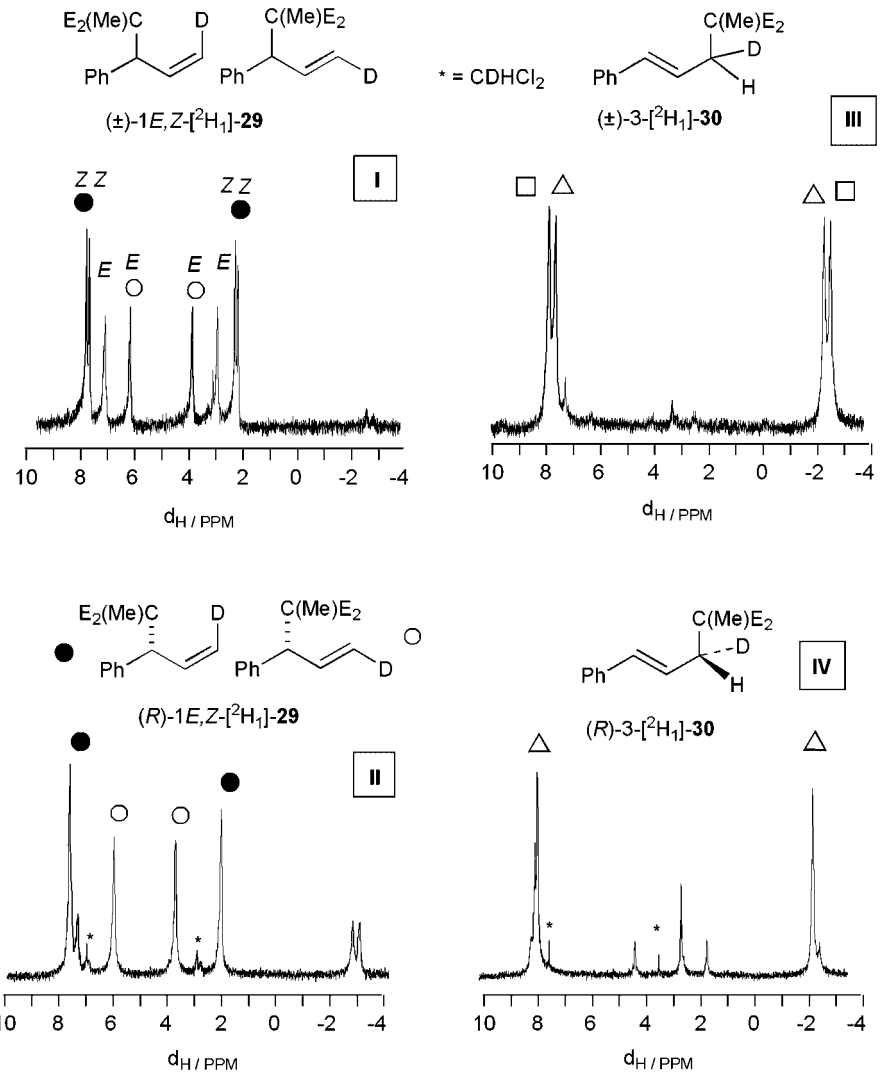

Scheme 21 ^{2}H{^{1}H}-NMR spectra of reference samples of **29** and **30** dissolved in a chiral liquid crystal matrix (CLCM).

DOI: 10.1002.jlcr

of challenging structures that we are willing to attempt to build. To set the scene, we end this paper with the structure of a chiral ligand (**32**). The ligand is decadeuterated (d_{10}) with two *P*-stereogenic centres, chiral by virtue of isotopic substitution, and thus has four stereogenic centres in total. We have completed a formal total synthesis of this molecule, as >97% a single diastereoisotopomer in >99% ee, in an 11-step synthesis starting from PCl_3, Scheme 23. This d_{10}-labelled system (and it's C_2-symmetric *P*-diastereoisotopomer) will soon provide us with the tools to explore the three-dimensional structure of Pd-allyl complexes of this ligand using NMR spectroscopy—a goal that has eluded us for over a decade.[27]

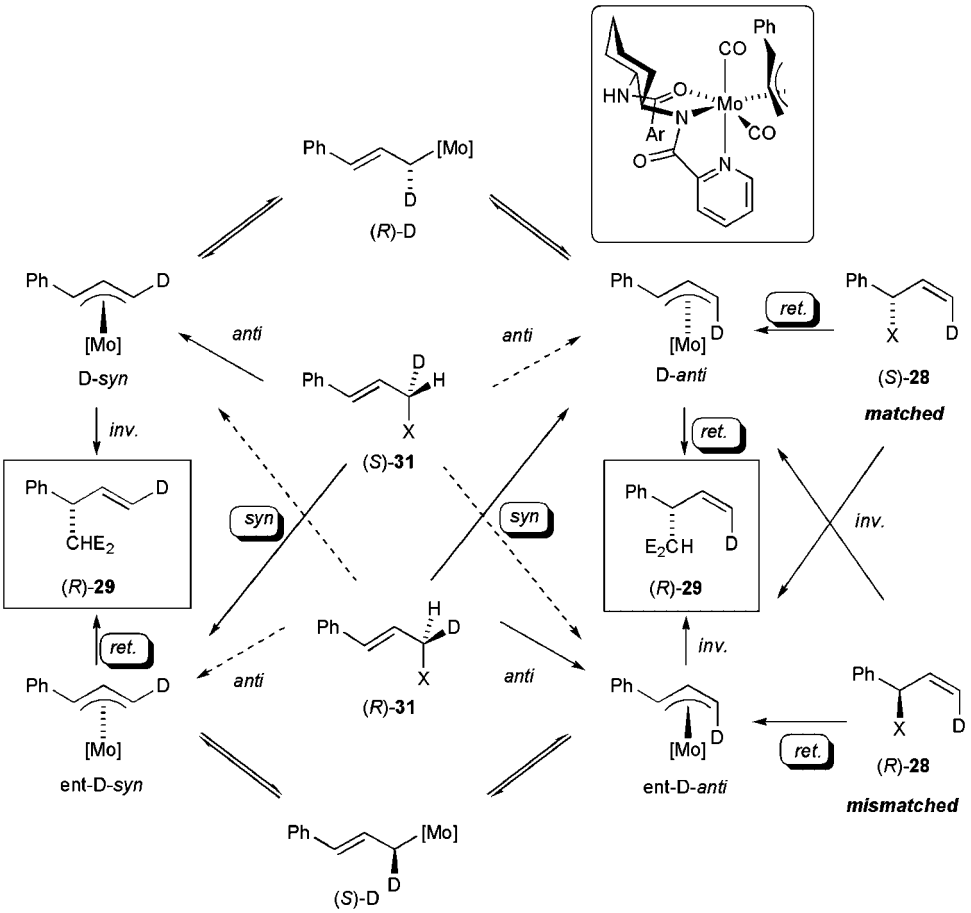

Scheme 22 Stereochemical outcome in Mo-catalysed allylation as deduced by $^{2}H\{^{1}H\}$ NMR spectroscopy in a CLCM, ^{1}H NMR nOe studies and X-ray crystallography of isolated intermediate allyl (shown).

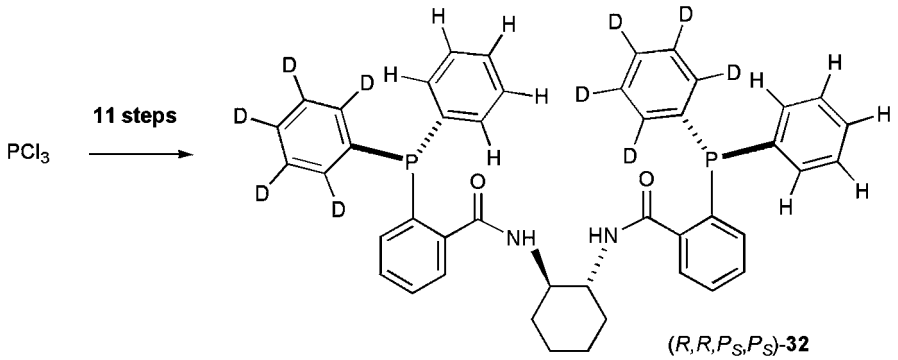

Scheme 23 .

DOI: 10.1002.jlcr

REFERENCES

1. Lloyd-Jones GC, Slatford PA. *J Am Soc* 2004; **126**: 2690–2691.
2. Reviews on 1,*n*-diene cycloisomerisation: (a) Trost BM, Krische MJ. *Synlett* 1998; 1–15; (b) Widenhoefer RA. *Acc Chem Res* 2002; **35**: 905–913; (c) Lloyd-Jones GC. *Org Biomol Chem* 2003; **1**: 215–236.
3. Bray KL, Fairlamb IJS, Charmant JPH, Lloyd-Jones GC. *Chem Eur J* 2001; **7**: 4205–4215.
4. Takacs JM, Lawson EC, Clement F. *J Am Chem Soc* 1997; **119**: 5956–5957.
5. Aggarwal VK, Fulford SY, Lloyd-Jones GC. *Angew Chem Int Ed* 2005; **44**: 1706–1708.
6. Baylis AB, Hillman MED. *Offenlegungsschrift* 2155113, 1972; U.S. Patent 3,743,669; *Chem Abstr* 1972; **77**: 34174q.
7. Hill JS, Isaacs NS. *J Phys Org Chem* 1990; **3**: 285–288.
8. Price KE, Broadwater SJ, Jung HM, McQuade, DT. *Org Lett* 2005: 147–150.
9. Park K-S, Kim J, Choo H, Chong Y. *Synlett* 2007; 395–398.
10. Alder RW, Lloyd-Jones GC, Owen-Smith GJJ. *Chem Eur J* 2006; **12**: 5361–5375.
11. For an extensive list of reviews of these remarkable compounds, see Reference [10].
12. Arduengo III. AJ, Calbrese JC, Davidson F, Dias HVR, Goerlich JR, Krafczyk R, Marshall WJ, Tamm M, Schmutzler R. *Helv Chim Acta* 1999; **82**: 2348–2364; (b) Sole S, Gornitzka H, Schoeller WW, Bourissou D, Bertrand G. *Science* 2001; **292**: 1901–1903; (c) Korotikh NI, Rayenko GF, Shvaika OP, Pekhtereva TM, Cowley AH, Jones JN, Macdonald CLB. *J Org Chem* 1993; **68**: 5762–5765; (d) Nyce GW, Csihony S, Waymouth RM, Hedrick JL. *Chem Eur J* 2004; **10**: 4073–4079.
13. Lloyd-Jones GC, Margue RG, de Vries JG. *Angew Chem Int Ed* 2005; **44**: 7442–7447.
14. Mori M, Sakakibara N, Kinoshita A. *J Org Chem* 1998; **63**: 6082–6083.
15. (a) Hoye TR, Donaldson SM, Vos TJ. *Org Lett* 1999; **1**: 277–279; (b) Schramm MP, Reddy DS, Kozmin SA. *Angew Chem Int Ed* 2001; **40**: 4274–4277; (c) Hansen EC, Lee D. *J Am Chem Soc* 2003; **125**: 9582–9583; (d) Sashuk V, Grela K. *J Mol Cat A* 2006; **257**: 59–66; (e) Lippstreu JJ, Straub BF. *J Am Chem Soc* 2005; **127**: 7444–7457.
16. Rendler S, Oestreich M, Butts C, Lloyd-Jones GC. *J Am Soc* 2007; **129**: 502–503.
17. (a) LaPointe AM, Rix FC, Brookhart M. *J Am Chem Soc* 1997; **119**: 906–917; (b) Perch NS, Widenhoefer RA. *J Am Chem Soc* 2004; **126**: 6332–6346.
18. (a) Bray KL, Lloyd-Jones GC. *Eur J Org Chem* 2001; 1635–1642; (b) Bray KL, Lloyd-Jones GC, Muñoz MP, Slatford PA, Tan EHP, Tyler-Mahon AR, Worthington PA. *Chem Eur J* 2006; **12**: 8650–8663.
19. (a) Charmant JPH, Dyke AM, Lloyd-Jones GC. *Chem Commun* 2003; 380–381; (b) Zhao Z, Messinger J, Schön U, Wartchow R, Butenschön H. *Chem Commun* 2006; 3007–3009.
20. Kargbo R, Takahashi Y, Bhor S, Cook GR, Lloyd-jones GC, Shepperson IR. *J Am Chem Soc* 2007; **129**: 3846–3847.
21. Dyke AM, Gill D, Harvey JN, Hester AJ, Lloyd-Jones GC, Munoz MP, Shepperson IR. Unpublished results.
22. (a) Charmant JPH, Lloyd-Jones GC, Peakman TM, Woodward RL. *Tetrahedron Lett* 1998; **39**: 4733–4736; (b) Charmant JPH, Lloyd-Jones GC, Peakman TM, Woodward RL. *Eur J Org Chem* 1999; **2**: 2501–2510; (c) Hodgson P, Lloyd-Jones GC, Murray M, Peakman TM, Woodward RL. *Chem Eur J* 2000; **6**: 4451–4460; (d) Lloyd-Jones GC, Harvey JN, Hodgson P, Murray M, Woodward RL. *Chem Eur J* 2003; **9**: 4523–4535.
23. Pietrzak M, Wehling J, Limbach HH, Golubev NS, Lopez C, Claramunt RM, Elguero J. *J Am Chem Soc* 2001; **123**: 4338–4339.
24. (a) Lloyd-Jones GC, Stephen SC. *Chem Commun* 1998: 2321–2322; (b) Lloyd-Jones GC, Stephen SC. *Chem Eur J* 1998; **4**: 2539–2549; (c) Fairlamb IJS, Lloyd-Jones GC, Vyskocil S, Kočovský P. *Chem Eur J* 2002; **8**: 4443–4453; (d) Gouriou L, Lloyd-Jones GC, Vyskocil S, Kočovský P. *J Organometall Chem* 2003; **687**: 525–537.
25. (a) Malkov AV, Gouriou L, Lloyd-Jones GC, Starý I, Langer V, Spoor P, Vinader V, Kočovský P. *Chem Eur J* 2006; **12**: 6910–6929; (b) Hughes DL, Lloyd-Jones GC, Krska SW, Gouriou L, Bonnet VD, Jack K, Sun R, Reamer RA. *Proc Natl Acad Sci* 2004; **101**: 5379–5384; (c) Lloyd-Jones GC, Krska SW, Hughes DL, Gouriou L, Bonnet, VD, Jack K, Sun Y, Reamer RA. *J Am Chem Soc* 2004; **126**: 702–703.
26. For an excellent overview of the technique, see: Sarfati M, Lesot P, Merlet D, Courtieu J. *Chem Commun* 2000; 2069–2081.
27. Lloyd-Jones GC, Stephen SC, Fairlamb IJS, Martorell A, Dominguez B, Tomlin PM, Murray M, Fernadez JM, Jeffery JC, Riis-Johannessen T, Guerziz T. *Pure Appl Chem* 2004; **76**: 589–601.